



# A reference methodology for microplastic particle size distribution analysis: Sampling, filtration, and detection by optical microscopy and image processing

Susanne Richter<sup>1</sup>  | Julia Horstmann<sup>1</sup> | Korinna Altmann<sup>2</sup> | Ulrike Braun<sup>3</sup>  | Christian Hagendorf<sup>1</sup>

<sup>1</sup>Fraunhofer Center for Silicon Photovoltaics CSP, Halle (Saale), Germany

<sup>2</sup>Bundesanstalt für Materialforschung und -prüfung BAM, Berlin, Germany

<sup>3</sup>Umweltbundesamt, Berlin, Germany

## Correspondence

Susanne Richter, Fraunhofer Center for Silicon Photovoltaics CSP, Otto-Eißfeldt-Str. 12, 06120 Halle (Saale), Germany.

Email: [susanne.richter@csp.fraunhofer.de](mailto:susanne.richter@csp.fraunhofer.de)

## Funding information

Projekt "RuSeKu", FKZ: 02WPL1442D, 02WPL1442A; Bundesministerium für Bildung und Forschung

## Abstract

Microplastic (MP) contamination in natural water circulation is a concern for environmental issues and human health. Various types of polymer materials have been identified and were detected in MP analytic test procedures. Beyond MP polymer type, particle size and form play a major role in water analysis due to possible negative toxicologic effects on flora and fauna. However, the correct quantitative measurement of MP size distribution over several orders of magnitude is strongly influenced by sample preparation, filtration materials and processes, and micro-analytical techniques, as well as data acquisition and analysis. In this paper, a reference methodology is presented aiming at an improved quantitative analysis of MP particles. An MP analysis workflow is demonstrated including all steps from reference materials to sample preparation, filtration handling, and MP particle size distribution analysis. Background-corrected particle size distributions (1–1000  $\mu\text{m}$ ) have been determined for defined polyethylene (PE) and polyethylene terephthalate (PET) reference samples. Microscopically measured particle numbers and errors have been cross-checked with the total initial mass. In particular, defined reference MP samples (PE, PET) are initially characterized and applied to filtration experiments. Optical microscopy imaging on full-area Si filters with subsequent image analysis algorithms is used for statistical particle size distribution analysis. To quantify the effects of handling and filtration, several blind tests with distilled water are carried out to determine the particle background for data evaluation. Particle size distributions of PE and PET reference samples are qualitatively and quantitatively reproduced with respect to symmetry, and maximum and cut-off diameter of the distribution. It is shown that especially MP particles with a radius of  $>50 \mu\text{m}$  can be detected and retrieved with high reliability. For particle sizes  $<50 \mu\text{m}$ , a significant interference with background contamination is observed. Data from blank samples allows a correction of background contaminations. Furthermore, for enhanced sampling statistics, the recovery of the initial amount of MP will be qualitatively shown. The results are intended as an initial benchmark for

This is an open access article under the terms of the Creative Commons Attribution-NonCommercial-NoDerivs License, which permits use and distribution in any medium, provided the original work is properly cited, the use is non-commercial and no modifications or adaptations are made.

© 2022 The Authors. *Applied Research* published by Wiley-VCH GmbH.

MP analytics quality. This quality is based on statistical MP particle distributions and covers the complete analytic workflow starting from sample preparation to filtration and detection. Microscopic particle analysis provides an important supplement for the evaluation of established spectroscopic methods such as Fourier-transform infrared spectroscopy or Raman spectroscopy.

#### KEYWORDS

drinking water, filtration, microplastics detection, quality control, statistical particle distribution

## 1 | INTRODUCTION

Microplastics (MPs), that is, plastic particles in the dimension of 1–1.000  $\mu\text{m}$  (ISO/TR 21960) are now observed as contamination in all environmental media (e.g., aquatic, terrestrial, atmospheric, biological samples) and products (e.g., sewage sludge, compost, and food).

In particular, the occurrence of numerous particle quantities in aqueous media is striking in a variety of studies [1, 2]: sewage treatment plant effluents, surface waters, and marine waters. Although the risks posed by these particles to ecosystems are not yet clear, the ubiquitous presence is arising high public concern. Detection of MP in groundwater, drinking water, or tap water is less clear [3, 4], but appears to be a more critical issue because of the potential for direct risk to human health. This also includes the presence of MP in bottled water.

The assessment of hazards or risks requires valid procedures. It turned out [5] that existing procedures often have to be evaluated critically because minimal requirements are not met with regard to sample handling, background contaminations, and analytical instrumentation. For example, in a large number of studies, the avoidance of contamination from air or insufficient cleaned lab equipment [6] can often lead to an overestimation of particle counts. On the other hand, agglomeration of particles or deposits on lab equipment can lead to underestimations of particle counts. The meaningful determination of blank values and recovery rates is often neglected.

The basis for a valid and standardized analytical approach is the introduction of an analytical reference procedure. This includes the use of defined reference samples, which allow a significant improvement in reproducibility as well as MP detection limits. A quantitative metrology requires, in addition to basic representative methods for sampling, preparation, and detection, a defined and reproducible analytical procedure, including all materials and processes in use. In addition to reference MP materials, the filters and laboratory conditions used in interaction with the final MP measurement play a central role in detection limits and statistical measurement control. Based on available reference and filtration materials (e.g., metal mesh [7], Si [8],  $\text{AlO}_x$  [9], polycarbonate filters [10]) and analytical instrumentation (e.g., Fourier-transform infrared spectroscopy [FTIR] [7–9, 11–14] and Raman spectrometry [8, 15, 16], thermal extraction desorption-gas chromatography/mass spectrometry [12, 13, 17, 18]), the central aspects of

analytical MP method development have been investigated in recent years [19].

In this paper, a methodology for a reference filtration process will be presented that allows the measurement of blank values and recovery rates for specific MP particle size classes. The procedure is intended as a comprehensive reference methodology for a quantitative assessment and evaluation of MP analysis workflows, determining MP particle numbers. The reference materials are composed of polymeric particles with a defined size distribution, pressed in water-soluble salt tablets. Those tablets can be solved in a defined water volume and subsequently filtered with an appropriate filter material. The subsequent detection process is based on an automated optical microscopic process and can be easily adapted by laboratories. Full filter area particle size distribution analysis allows the determination of blank values and recovery rates for specific MP particle size classes. In the first instance, a qualitative assessment of the recovery rate for the used reference materials is obtained.

## 2 | THE FUNDAMENTAL MP ANALYTICS WORKFLOW

For quantitative measurements of the amount and type of MP particles in water, reliable lab routines and materials are essential. The workflow for MP analytics can be divided basically into three steps: sampling including sample preparation, filtration procedure, and detection. A typical workflow is schematically shown in Figure 1 with subroutines for each step.

The initial preparation of samples is the basis for all subsequent steps. Specific sampling methods are designed according to the analytical task, for example, drinking water analysis to provide the analytical sample. However, the implementation of blank and reference samples is mandatory for monitoring influences of handling and contaminations from lab and filtration equipment. For quantitative analysis, reference samples for the specific MP are required. Thus, a trustworthy test routine is based on at least three samples: the analytical sample, a blank sample for background contamination monitoring, and a reference sample for quantification purposes (see also Sections 3.1–3.3).

In the second stage, the filtration procedure and the involved materials are of major importance for reproducible MP particle size



**FIGURE 1** Workflow for microplastic analysis

distribution analysis. Water with MP has been filtered with various commercial or home-built filter setups. Beyond selecting the appropriate filter material, the filtration procedure demands defined conditions with regard to clean lab environments, filtration setup preparation, sample handling, and final drying of the filter substrate (see also Sections 3.4–3.7).

Finally, quantitative results for MP particle size distribution have to be acquired at the analytical stage. In previous publications, several methods ranging from high-resolution optical microscopy or spectroscopy (Raman, FTIR) have been used [9, 12]. To determine particle sizes down to a few micrometers, an adequate spatial resolution is required. Furthermore, a representative number of particles has to be analyzed to achieve a statistical information for particle size distribution, which is defined by the number of particles in a given range of size. In our approach, we focus on optical microscopy applied in stitching mode on homogeneously flat Si filter substrates with a size of several millimeters in diameter (Sections 3.8). In combination with image processing particle detection algorithms, a sufficient statistical information is obtained for a thorough discussion of errors and limits of detection in the presented analytics workflow. Additional information on polymer types may be obtained by correlative imaging strategies in combination with FTIR spectrometry [7–9, 11–14].

## 3 | EXPERIMENTAL

### 3.1 | Test preparation and laboratory environment

A clean laboratory environment and equipment are fundamental requirements when carrying out filtration tests for the detection of MP particles in water down to a size of  $<10\ \mu\text{m}$ . In our investigation, a standard lab environment has been chosen. The laboratory environment is reflected in the background values (blank sample) and holds further potential for optimization (e.g., experimenting in a clean room). Here, the optimized workflow of a realistically clean laboratory environment was investigated. The particle load is measured by analysis of the blank sample. Filter materials and filtration equipment are cleaned before each filtration experiment. The filter material is cleaned with compressed air and rinsed with distilled water. Optical microscopy using darkfield contrast up to  $\times 20$  magnification of the filter surface is performed before filtration for documentation and to determine the

**TABLE 1** Initial and measured TGA mass content of PET and PE (aged) polymer per KBr tablet

MP type	Initial MP mass ( $\mu\text{g}$ )	Measured TGA mass ( $\mu\text{g}$ ) (n = 10)
PET	1490	$1850 \pm 1100$ (60.1%)
PE (aged)	149	$126 \pm 22.5$ (17.8%)

Note: The homogeneity of the polymer and KBr mixture has been checked by measuring 10 tablets.

Abbreviations: MP, microplastic; PE, polyethylene; PET, polyethylene terephthalate; TGA, thermogravimetric analysis.

limits of detection that are determined by environmental particle contaminations. In general, a particle background needs to be detected by microscopic inspection of the used Si filter after blank sample filtration. Furthermore, filtration equipment is rinsed under running water for approximately 1 min, cleaned with deionized (DI) water, and dried with compressed air.

### 3.2 | MP reference materials

MP reference powder was prepared by cryo grinding from polyethylene terephthalate (PET) granulates and aged polyethylene (PE) foils at BAM labs (Bundesanstalt für Materialforschung). Reference material tablets were fabricated by mixing and pressing in a KBr matrix with a total mass of 250 mg. In this investigation, MP suspensions have been prepared from KBr tablets with a mass of  $149\ \mu\text{g}$  PE and  $1490\ \mu\text{g}$  PET per 250 mg tablet, respectively.

Additionally, the mass homogeneity of the KBr MP mixture was checked by thermogravimetric analysis (TGA) regarding the mass content per KBr tablet for a representative number of 10 tablets. The initial mass and the measured TGA mass of PET and aged PE per tablet are shown in Table 1. It should be noted that the MP mass content in PET and aged PE tablets differ by a factor of 10. Furthermore, the variation in measured TGA mass is up to 60% for PET KBr tablets.

### 3.3 | Sampling/sample preparation

Any MP sample to be analyzed should of course be handled without the use of additional plastic vessels. For the preparation of liquid MP

solutions for subsequent filtration experiments, the tablets have been dissolved in DI water (<30–100 ml) within glass vessels. As a blank sample, distilled water of the same volume has been used without any additives (e.g., ethanol, surfactant).

### 3.4 | Filtration equipment

Equipment used for MP particle size distribution analysis in this publication comprises glass beakers for the preparation of the liquid solution of the MP reference material, stainless-steel filter hoppers and Si filters, and adapters as described below. To avoid MP cross-contaminations, it is important that any material in this setup is made of nonplastic material. In our experiments, vessels from commercial lab suppliers (e.g., Sartorius) have been used. Alternatively, commercial MP filtration equipment made of glass (Bruker Optics GmbH) was used [20]. For the implementation of Si filters, a nonplastic adapter kit made of components of aluminum and brass with copper gaskets has been developed and used at Fraunhofer CSP.

### 3.5 | Silicon filters

To achieve a filtration cut-off at particle diameter <10  $\mu\text{m}$ , various filter materials are applied in MP analytics [8–10]. For particle size distribution measurement, large-area optical microscopy and microspectroscopy methods (FTIR, Raman) are widely used. These final MP analytic methods require a high planarity of the filter substrate (roughness <10 nm), an optical homogeneity at a length scale <10  $\mu\text{m}$ , and appropriate optical transmission/reflection properties

for particle analysis. Especially, a transmittance in the IR range >1000 nm is important to detect characteristic absorption bands from the polymers. In our experiment, Si filters have been used. Macroporous Si filters were obtained from SmartMembranes GmbH [21]. Pore sizes of 10  $\mu\text{m}$  and filter thickness of 300  $\mu\text{m}$  have been used. Macroporous Si substrate provides a high contrast for most MPs species in darkfield optical microscopy. Due to the elevated porosity, some spectroscopic artifacts are observed due to scattering and oxidic surface layers.

Si filters were also fabricated by laser micromachining of double-side polished wafer material. This filter substrate was developed at Fraunhofer CSP [22]. As shown in Figure 2, the pore size is down to 25  $\mu\text{m}$  and can be processed with variable possible pitch geometries of 100–500  $\mu\text{m}$ . The shown Si filters have nominal pore sizes of 90  $\mu\text{m}$  (Figure 2a) and 25  $\mu\text{m}$  (Figure 2b), depicted in the same optical magnification. The reduced number of pores in comparison to some macroporous Si geometries leads to an improved spectral IR transmittance.

Alternatively,  $\text{AlO}_x$  filters (Anodisc™) provided by Whatman™ (Cytiva) are commonly used in some labs as an inorganic substrate for microscopy applications. However, due to the optical properties of  $\text{AlO}_x$ , some limitations in the bandwidth of the spectral transmission are observed, which are critical for FTIR analytics of some polymer materials (data not shown).

### 3.6 | Filtration process and drying

In a typical filtration process, the dissolved MP reference sample is poured through a funnel that holds the filter within a stainless-steel adapter. For the given conditions, additional pressure or vacuum will

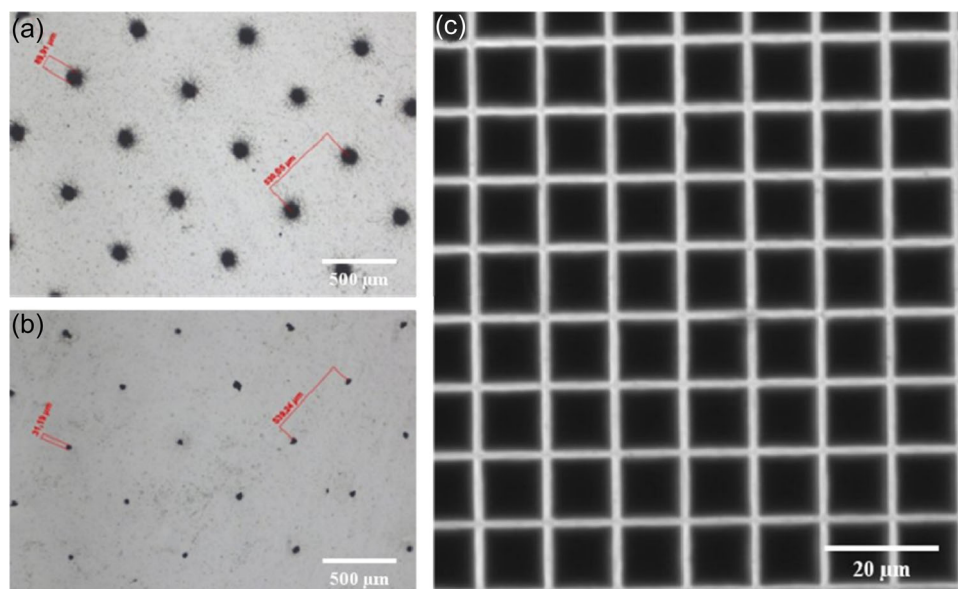


**FIGURE 2** Optical microscopy image of laser processed Si filters (pore size from 90  $\mu\text{m}$  down to 25  $\mu\text{m}$ ) (a, b) and electrochemically etched Si filter produced by SmartMembranes GmbH (pore size 10  $\mu\text{m}$ ) (c) before filtration.

not be required for the filtration of 300 ml liquid within 30 s. Before and after the use of the filter setup, the system must be kept clean and dust-free by adequate cleaning and rinsing. After cleaning the filter setup, the blank sample should be filtered first. Then, the sample to be analyzed and the reference sample is filtered through the setup (each with a new filter). The beaker is rinsed with distilled water 2–3 times to remove excess particles. The liquid is also poured through the filter. To protect the filter from particles in the air a glass cap is used for covering the funnel cone during the filtration process. After filtration, the filter and the adapter are placed on a heating plate at 50°C for around 4–8 h for drying. Again, air-borne dust coverage is mandatory. Furthermore, residual water and humid air have to be allowed to escape the setup by loosening some parts. Flipping of the filter during filtration or handling should be prevented. If the filter is still wet after removing it from the adapter, an additional heating at 50°C may be required.

### 3.7 | Analytical instrumentation

Optical microscopy was performed using a Zeiss Axio.Scope A1 device in reflected light darkfield contrast mode. Mapping of the whole filter is created with a motorized stage by stitching single frames together. Subsequently, optical microscopy was used in high resolution and with five fold magnification (Figure 4). For image detection, a black/white camera with 255 gray values was implemented. Image stitching has been performed to map the complete filter surface. Stitching was optimized by software algorithms using 3% overlap for the single images to prevent errors at the overlapping edges of the images.

### 3.8 | Image processing and particle detection algorithms

The mapping of the detected particle distribution of filter material after the filtration procedure needs to be image processed by the software, like ImageJ [23] using a macro with defined parameters. By including information such as grayscale, circularity threshold, particle size, and pore size, the program is able to detect the particles and measure their size. Particle size and the density of the identified MP species (e.g., PE or PET) are used to calculate the total mass of MP. ImageJ macro gives small and large ellipse axis. The particle volume is approximated as an ellipsoid and the mass calculation takes this into account.

## 4 | RESULTS AND DISCUSSION

### 4.1 | Initial MP particle size distribution of PE and PET reference materials

The initial particle size distribution of the analyzed material as measured by laser diffraction is exemplarily shown for PET and PE

(aged) in Figure 3. PET particle size distribution appears slightly asymmetric in logarithmic plotting of the x-axis and is slightly shifted to larger particle sizes. The maximum particle distribution is achieved for a particle size of 255  $\mu\text{m}$ . Also, aged PE particles are asymmetrically distributed with a maximum particle size of 68  $\mu\text{m}$  shifted to smaller particle sizes. The maximum particle size observed for both distributions is similar at a particle size of  $\sim 300 \mu\text{m}$ .

Various characteristic parameters can be derived from laser diffraction data and implemented for the statistical description of the particle size distribution. As summarized in Table 2, for comparison with optical microscopy particle counting (Sections 4.2 and 4.3), the most important parameters are the particle size values for the distribution maximum (PS-DM) and the upper cut-off particle size (PS-UCO) of the distribution. The smallest detected particle sizes are at  $<1$  and 5–10  $\mu\text{m}$  for PE (aged) and PET, respectively.

For mass analysis, an average particle diameter PS-D50 is calculated indicating the mass median diameter D50. It is obvious that for the symmetric aged PE distribution PS-DM and PS-D50 values coincide at 60–70  $\mu\text{m}$ , whereas in the asymmetric PET distribution, values of 255 and 174  $\mu\text{m}$  are obtained, respectively. This has to be taken into account for further discussing particle statistics based on particle counting techniques or mass analysis approaches.

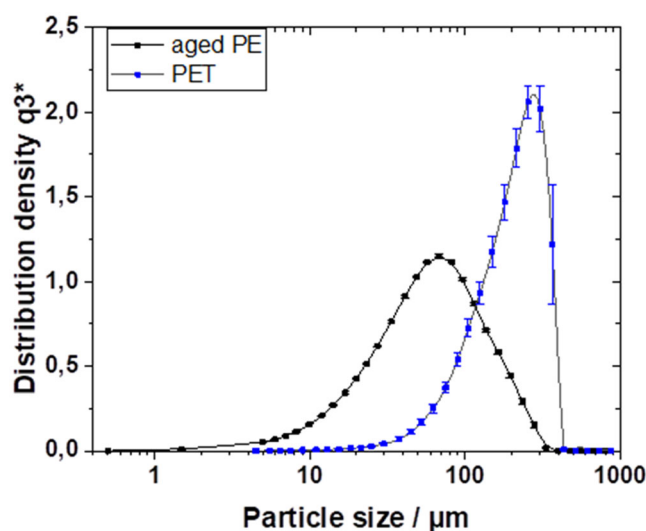


**FIGURE 3** PET (blue) and aged PE (black) particle size distribution assuming spherical particles measured by laser diffraction. PE, polyethylene; PET, polyethylene terephthalate.

**TABLE 2** Characteristic particle sizes for PE (aged) and PET at PS-DM, PS-UCO, and PS-D50

MP type	PS-DM ( $\mu\text{m}$ )	PS-UCO ( $\mu\text{m}$ )	PS-D50 ( $\mu\text{m}$ )
PET	255	440	174 $\pm$ 4
PE (aged)	68	330	60.67 $\pm$ 0.54

Abbreviations: MP, microplastic; PE, polyethylene; PET, polyethylene terephthalate; PS-D50, particle size D50 mass distribution; PS-DM, particle size at distribution maximum; PS-UCO, upper cut-off particle size.

## 4.2 | Large-area optical microscopy and particle detection

Filtration experiments were performed according to the procedure described in Section 3. Figure 4 shows a Si filter (with a pore size of  $10\ \mu\text{m}$ ) for filtration of KBr-PE reference material suspension in distilled water via optical microscopy. The particles are homogeneously distributed on the Si filter (Figure 4a). After the application of the particle detection algorithm, the detected particles are marked by red outlines (Figure 4b). Particle detection allows the reliable identification of particles down to  $50\ \mu\text{m}$ , with a minimum particle size of  $>20\ \mu\text{m}$  (see Figure 5c). The signal background of the filter is low and mainly refers to small particles with sizes  $<20\ \mu\text{m}$ . The type and composition of the impurity particles cannot be clearly identified, but the majority of the particles show the characteristic irregularly shaped outline of PET. The identification of characteristic PE and PET particles for the individual experiments was confirmed by FTIR and Raman spectroscopy (not shown here) showing the characteristic spectra. However, for time limitations of the measurements, only small sections of the filters can be measured with these spectral methods with high spatial resolution, and therefore a comparison of absolute particle counts for a complete filter is not practical. In the case of homogeneous particle distributions over filter surfaces, the results for the measurable particle numbers per area (in particular for  $\mu\text{Raman}$  spectroscopy) are consistent.

Analogous to PE also PET reference material was handled following the filtration procedure. PET particles are homogeneously distributed. In contrast to PE, the PET particles are larger in size (see Figure 5); individual particles with a maximum size of up to  $\sim 300\ \mu\text{m}$  are identified, this coincides with the asymmetry and sharp cutoff in the initial distribution. Particle detection allows the reliable identification of particles down to  $50\ \mu\text{m}$ , with a minimum particle size of  $>20\ \mu\text{m}$  (see Figure 5c). The signal background of the filter is low and mainly refers to small particles with sizes  $<20\ \mu\text{m}$ . The type and composition of the impurity particles cannot be clearly identified, but the majority of the particles show the characteristic irregularly shaped outline of PET. The identification of characteristic PE and PET particles for the individual experiments was confirmed by FTIR and Raman spectroscopy (not shown here) showing the characteristic spectra. However, for time limitations of the measurements, only small sections of the filters can be measured with these spectral methods with high spatial resolution, and therefore a comparison of absolute particle counts for a complete filter is not practical. In the case of homogeneous particle distributions over filter surfaces, the results for the measurable particle numbers per area (in particular for  $\mu\text{Raman}$  spectroscopy) are consistent.

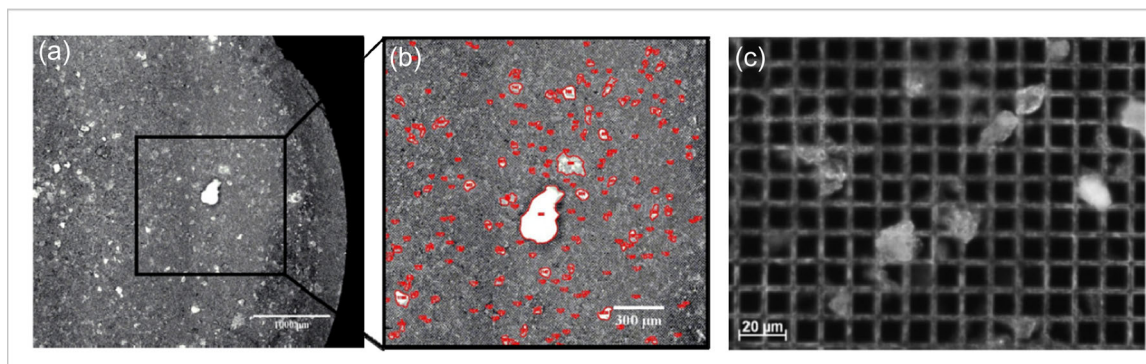


**FIGURE 4** Microscopic mapping of Si filter (SmartMembranes,  $10\ \mu\text{m}$  pore size) after PE filtration procedure (a) with the marked section of identified particles detected by ImageJ algorithm (b) and detail of optical microscopy of the filtered PE particles (c). PE, polyethylene.

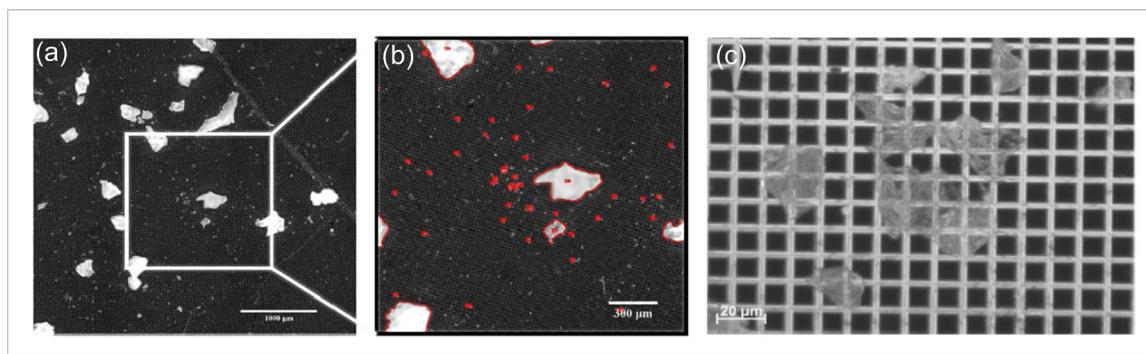


**FIGURE 5** Microscopic mapping of Si filter (SmartMembranes,  $10\ \mu\text{m}$  pore size) after PET filtration procedure (a) with the marked section of identified particles detected by ImageJ algorithm (b) and detail of optical microscopy of the filtered PET particles (c). PET, polyethylene terephthalate.

### 4.3 | Particle size distribution data analysis

Large-area optical microscopy of highly planar Si filters is used to examine particle size distributions of PE and PET samples after filtration. Image analysis algorithms with the help of ImageJ macro for particle detection are applied for obtaining representative statistics. From the data analysis, the number of particles detected within the defined size classes according to the small ellipse axis is received. In the following, obtained particle size class distributions are shown for the PE and PET reference filtration results and given as the average distribution of five and six separate experiments, respectively. Error bars indicate the uncertainties of each measurement and data processing as well as the deviations of the individual histograms.

As visible in Figure 6, a strong maximum is observed in both histograms with 1400 counts for PE and 300 counts for PET for particle sizes from 10 to 50  $\mu\text{m}$ . This pronounced maximum does not agree with the expected particle size distribution for the initial PE and PET material (Figure 3). Furthermore, particle size classes from 10 to 50  $\mu\text{m}$  show large error bars of more than 100% for PE. However, the asymmetric PET distribution with a maximum of  $\sim 250 \mu\text{m}$  is reproduced in the second maximum for the size class 100–500  $\mu\text{m}$  of PET (Figure 6, right). In contrast, a more symmetric distribution without any cut-off is found for the PE filtration experiment (Figure 6, left). The expected maximum at  $\sim 50 \mu\text{m}$  interferes with the strong maximum (1400 particles) for the size class 10–50  $\mu\text{m}$ .

To measure background and cross-contamination particle counts as a function of particle size classes, blank sampling has been performed for samples from KBr tablets without MP (Figure 7a) and blank samples of distilled water (Figure 7b). In both experiments, a pronounced particle count of 200–300 particles is observed in size class 10–50  $\mu\text{m}$ . In other size classes, particle numbers ranging below 20 particles can be neglected for particle sizes  $>100 \mu\text{m}$ . Potential

sources of background contaminations may be related to air-borne dust particles.

From various experiments, it has been concluded that blind values (obtained by distilled water filtrations) are relatively stable for our lab environment and are not significantly influenced by KBr tablets. Thus, we assumed blank value subtraction as a useful strategy for data correction of raw sampling data in Figure 6 predominantly in size class 10–50  $\mu\text{m}$ .

Particle size class distributions after subtraction of the averaged blind value particle counts ( $n = 3$ ) in the individual size classes yield particle statistics as shown in Figure 8 for PE and PET, respectively. For PE, a reduced maximum of 1100 particles are obtained in size class 10–50  $\mu\text{m}$ . Referring to the maximum of the initial PE distribution at PS-DM = 68  $\mu\text{m}$ , we obtained a qualitatively representative PE distribution after filtration. For the PET distribution (initial maximum at PS-DM = 255  $\mu\text{m}$ ), the asymmetric appearance with an absolute maximum in the particle class of 100–500  $\mu\text{m}$  is confirmed. Particles below 5–10  $\mu\text{m}$  in size will not be detected due to the used filter pore size of 10  $\mu\text{m}$ .

### 4.4 | Measurement errors and plausibility assessment of PE and PET recovery

With regard to single MP analytic experiments, the main source of errors is the adhesion of MP particles to the filtration setup. A lower density of MP leads to the floating of particles on the surface of water. While the water level decreases during filtration, the particles may stick to the funnel and accumulate on the adapter. The same effect may occur in the beaker, where the MP is dissolved. The issue is reduced by rinsing the beaker and the filtration set up multiple times with DI water through the filter. Additionally, an impeding

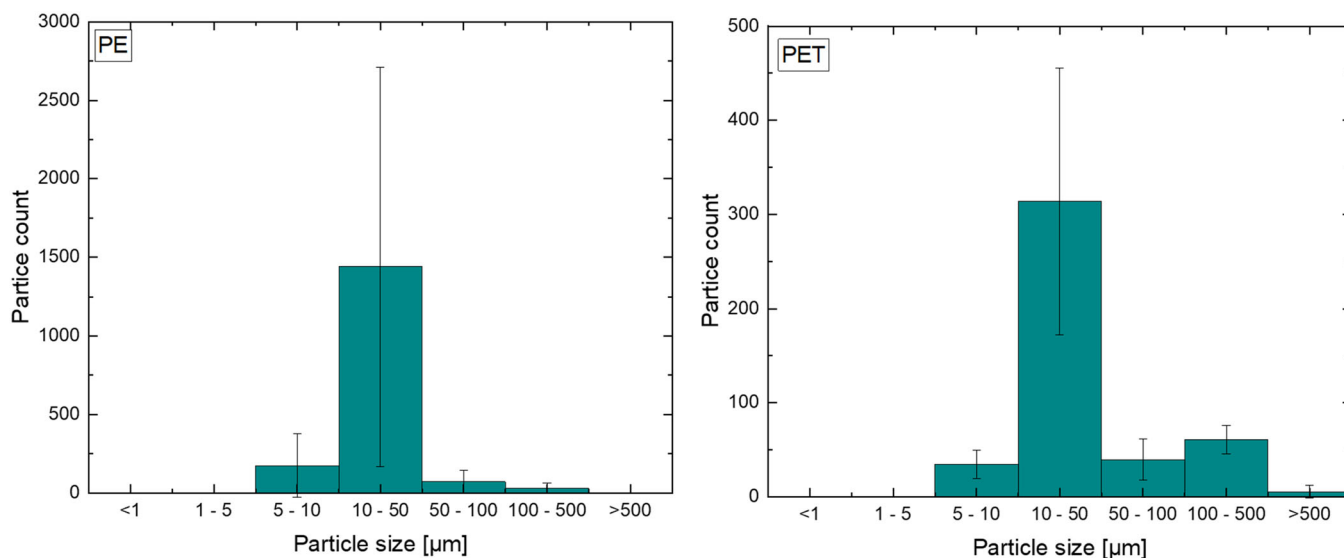


**FIGURE 6** PE (left) and PET microscopic particle statistics (right) of predefined reference material averaged over individual filtration experiments ( $n = 6$ ) for each particle size class. PE, polyethylene; PET, polyethylene terephthalate.

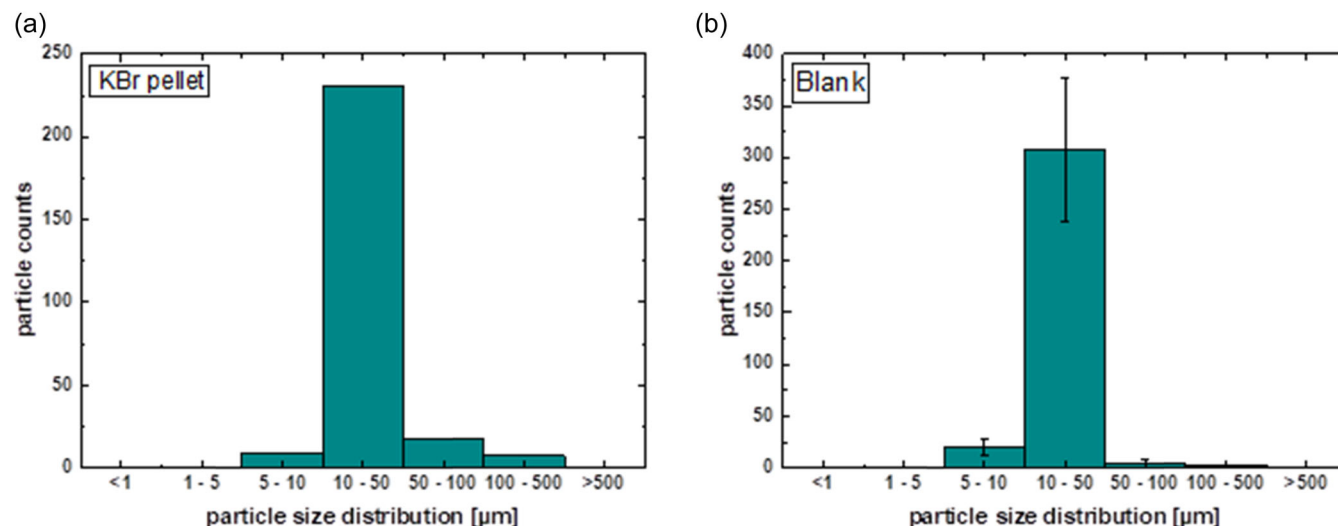


**FIGURE 7** Microscopic particle statistics of blank sampling (a) of KBr tablet without incorporated microplastic particles and (b) averaged blank samples of distilled water ( $n = 3$ ).

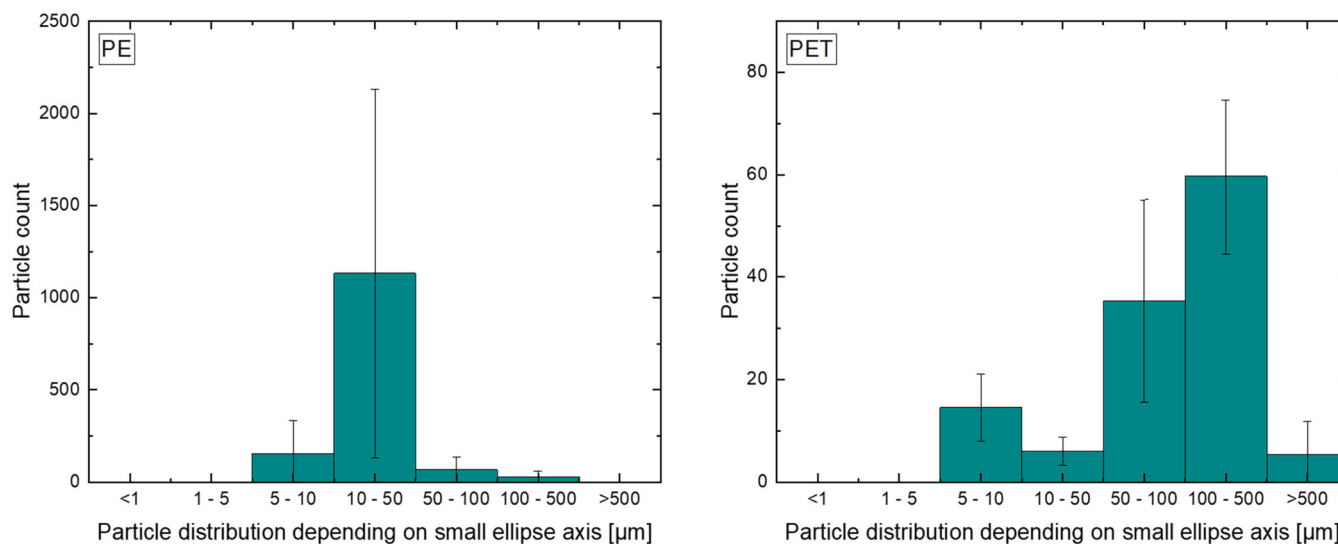


**FIGURE 8** PE and PET particle size class distribution after subtraction of blind value particle counts from blank solutions (see also Figure 7b). PE, polyethylene; PET, polyethylene terephthalate.

phenomenon is the adhesion of particles to each other, which may result in clustering on top of the filters. The analysis of the mapping with the software is hampered since the size of the particles in some cases cannot be determined correctly.

In this paper, a number of six independent MP analytics experiments for PE and PET have been performed for further MP data analysis. Based on the obtained PE and PET particle size distribution data, an extended analysis has been performed and related to blind sampling data.

The recovery rate is defined as the ratio of measured versus the initial mass of all MP particles. The total initial mass of PE and PET particles in the KBr tablets has been assumed as a reference. The total retrieval mass has been calculated from the sum of all individual

particles based on their elliptical volume and density. To achieve a statistical significance, six filtration samples of each polymer type, PE and PET, have been performed and analyzed.

In detail, the following assumptions have been made for data evaluation: (1) Standard polymer density values are given for PE at  $0.925 \text{ g/cm}^3$  and PET at  $1.39 \text{ g/cm}^3$  [24, 25]. (2) Particle volume is calculated as ellipsoid since the ImageJ algorithm provides small and large ellipse axis for each detected particle. (3) Number of particles in each size class is determined after blind value subtraction as shown in Figure 8.

Table 3 represents the total number of particles, the total initial mass, the total retrieved mass after filtration, and the obtained recovery rate for PE and PET distribution. Furthermore, the total



**TABLE 3** PE and PET total initial and retrieval mass as well as calculated recovery rates for six PE and PET filtration samples, each

	Total number of particles	Size distribution (D50)	Total initial mass measured by TGA in KBr tablet ( $\mu\text{g}$ )	Total retrieved mass after filtration, calculated ( $\mu\text{g}$ )	Recovery rate
PE	1699	70	126 $\pm$ 23 (17.8%)	143 $\pm$ 109 (76.5%)	1.175
PET	448	50	1850 $\pm$ 1100 (60.1%)	1853 $\pm$ 1457 (78.6%)	1.005
Blank	333	20	-	5.1	-

Note: The calculated mass for the average blank sample is given at the bottom.

Abbreviations: PE, polyethylene; PET, polyethylene terephthalate; TGA, thermogravimetric analysis.

mass of blind samples (assuming  $1\text{ g/cm}^3$ ) has been calculated. The data are obtained from an average of six PE and PET samples, each. As a plausibility check for the experiments performed in this paper, the total recovery rate for PET is close to 1, whereas the recovery rate is at 1.175 for PE. The error in total mass induced by the particles ( $\sim 5.1\ \mu\text{g}$ ) from the blank sample is relatively low—this is probably due to the small background particle sizes.

It should be noted that the obtained PE and PET calculated recovery rates are of qualitative character due to the high statistical errors in particle counting. Furthermore, systematic errors have to be considered due to simplified assumptions in the mass calculation (e.g., deviations from elliptical particle shape). However, the basic agreement of MP analysis data derived from mass and from particle analysis can be plausibly shown within the given limits of detection for an enhanced number of six filtration samples. Furthermore, a strong influence of the characteristic PE and PET size distributions is observed.

## 5 | CONCLUSION

A reference methodology is investigated in this study, aiming at an improved quantitative analysis of MP particles. An MP analysis workflow is presented including all steps from reference materials to sample preparation, filtration handling, and MP particle size distribution analysis. Background-corrected particle size distributions (1–1000  $\mu\text{m}$ ) have been determined for defined PE and PET reference samples. Microscopically measured particle numbers and errors have been cross-checked with the total initial mass.

Reference MP samples (PE, PET) were initially characterized with regard to their specific particle size distribution as well as total mass using laser diffraction and TGA. KBr tablets have been fabricated with high MP homogeneity and applied in filtration experiments on Si filter substrates. Optical microscopy imaging of full-area filter substrates with subsequent image analysis algorithms was implemented for statistical particle size distribution analysis. Blind tests with distilled water were carried out to determine the specific particle background originating from sample handling. Microscopic image analysis after filtration experiments could reproduce PE and PET particle size distribution both qualitatively and quantitatively with respect to symmetry, maximum, and cut-off diameter. MP particles with a radius of  $>50\ \mu\text{m}$  can be detected and retrieved with high

reliability. Particle sizes  $<50\ \mu\text{m}$  exhibit a significant interference with background contaminations that could be corrected by using data from blank samples. The recovery of the initial amount of MP could be qualitatively shown by the order of magnitude.

## ACKNOWLEDGMENTS

We like to thank Jakob Schick for his support in creating the ImageJ macro and Steffi Göller for her work on the filtration experiments. Financial support by the Federal Ministry of Education and Research-funded project RUSEKU (FKZ 02WPL1442D, 02WPL1442A) is gratefully acknowledged. Open Access funding enabled and organized by Projekt DEAL.

## CONFLICT OF INTEREST

The authors declare no conflict of interest.

## DATA AVAILABILITY STATEMENT

The data that support the findings of this study are available from the corresponding author upon reasonable request.

## ORCID

Susanne Richter  <http://orcid.org/0000-0002-4190-9144>

Ulrike Braun  <http://orcid.org/0000-0002-3682-3637>

## REFERENCES

- [1] L. Yang, Y. Zhang, S. Kang, Z. Wang, C. Wu, *Sci. Total Environ.* **2021**, 754, 141948.
- [2] W. Liu, J. Zhang, H. Liu, X. Guo, X. Zhang, X. Yao, Z. Cao, T. Zhang, *Environ. Int.* **2021**, 146, 106277.
- [3] S. M. Mintenig, M. G. J. Löder, S. Primpke, G. Gerdt, *Sci. Total Environ.* **2019**, 648, 631.
- [4] P. Alexy, E. Anklam, T. Emans, A. Furfari, F. Galgani, G. Hanke, A. Koelmans, R. Pant, H. Saveyn, B. Sokull Kluttgen, *Food Addit. Contamin. Part A* **2020**, 37(1), 1.
- [5] A. A. Koelmans, N. H. Mohamed Nor, E. Hermsen, M. Kooi, S. M. Mintenig, J. De France, *Water Res.* **2019**, 155, 410.
- [6] C. Wesch, A. M. Elert, M. Wörner, U. Braun, R. Klein, M. Paulus, *Sci. Rep.* **2017**, 7(1), 5424.
- [7] S. Ziajahromi, P. A. Neale, L. Rintoul, F. D. L. Leusch, *Water Res.* **2017**, 112, 93.
- [8] A. Käppler, F. Windrich, M. G. J. Löder, M. Malanin, D. Fischer, M. Labrenz, K.-J. Eichhorn, B. Voit, *Anal. Bioanal. Chem.* **2015**, 407(22), 6791.
- [9] A. J. Negrete Velasco, L. Rard, W. Blois, D. Lebrun, F. Lebrun, F. Pothe, S. Stoll, *Water* **2020**, 12(9), 2410.

- [10] C. Zhu, Y. Kanaya, R. Nakajima, M. Tsuchiya, H. Nomaki, T. Kitahashi, K. Fujikura, *Environ. Pollut.* **2020**, 263(Pt B), 114296.
- [11] J. P. G. L. Frias, V. Otero, P. Sobral, *Mar. Environ. Res.* **2014**, 95, 89.
- [12] E. Hendrickson, E. C. Minor, K. Schreiner, *Environ. Sci. Technol.* **2018**, 52(4), 1787.
- [13] A. Käppler, M. Fischer, B. M. Scholz-Böttcher, S. Oberbeckmann, M. Labrenz, D. Fischer, K.-J. Eichhorn, B. Voit, *Anal. Bioanal. Chem.* **2018**, 410(21), 5313.
- [14] Y. Chen, D. Wen, J. Pei, Y. Fei, D. Ouyang, H. Zhang, Y. Luo, *Curr. Opin. Environ. Sci. Health* **2020**, 18, 14.
- [15] B. E. Oßmann, G. Sarau, S. W. Schmitt, H. Holtmannspötter, S. H. Christiansen, W. Dicke, *Anal. Bioanal. Chem.* **2017**, 409(16), 4099.
- [16] L. van Cauwenberghe, A. Vanreusel, J. Mees, C. R. Janssen, *Environ. Pollut.* **2013**, 182, 495.
- [17] C. G. Bannick, R. Szewzyk, M. Ricking, S. Schniegler, N. Obermaier, A. K. Barthel, K. Altmann, P. Eisentraut, U. Braun, *Water Res.* **2019**, 149, 650.
- [18] E. Dümichen, A.-K. Barthel, U. Braun, C. G. Bannick, K. Brand, M. Jekel, R. Senz, *Water Res.* **2015**, 85, 451.
- [19] A. M. Elert, R. Becker, E. Duemichen, P. Eisentraut, J. Falkenhagen, H. Sturm, U. Braun, *Environ. Pollut.* **2017**, 231(Pt 2), 1256.
- [20] Bruker Optics GmbH. *Product Note M184: A165-MP Filtration Set for Microplastic Analysis and Sample Preparation*, Bruker Optics GmbH, **2019b**.
- [21] SmartMembranes GmbH. *MakroPor: Macroporous Silicon FactSheet*, SmartMembranes GmbH, Stuttgart, Germany, **2019a**.
- [22] C. Hagendorf, K. Kaufmann, U. Braun, inventors. Filter substrate for filtering and optically characterizing microparticles, method for producing the filter substrate, and use of the filter substrate. US patent #20210364405, **2019**.
- [23] M. D. Abràmoff, P. J. Magalhães, S. J. Ram, *Biophoton. Int.* **2004**, 11(7), 36.
- [24] W. Caseri, K. Beutner, *Polyethylene*, Thieme Gruppe, Stuttgart, Germany, **2009a**.
- [25] W. Caseri, K. Beutner, *Polyethylenterephthalate*, Thieme Gruppe, Germany, **2009b**.

**How to cite this article:** S. Richter, J. Horstmann, K. Altmann, U. Braun, C. Hagendorf, *Appl. Res.* **2022**, e202200055.  
<https://doi.org/10.1002/appl.202200055>